2010 IEEE International Conference on Robotics and Automation
Anchorage Convention District
May 3-8, 2010, Anchorage, Alaska, USA

Novel Miniature MRI-Compatible Fiber-Optic Force Sensor for Cardiac Catheterization Procedures

Panagiotis Polygerinos, *Graduate Student Member, IEEE,* Pinyo Puangmali, Tobias Schaeffter, Reza Razavi, Lakmal D. Seneviratne, *Member, IEEE* and Kaspar Althoefer, *Member, IEEE*

***Abstract*— This paper presents the prototype design and development of a miniature MR-compatible fiber optic force sensor suitable for the detection of force during MR-guided cardiac catheterization. The working principle is based on light intensity modulation where a fiber optic cable interrogates a reflective surface at a predefined distance inside a catheter shaft. When a force is applied to the tip of the catheter, a force sensitive structure varies the distance and the orientation of the reflective surface with reference to the optical fiber. The visual feedback from the MRI scanner can be used to determine whether or not the catheter tip is normal or tangential to the tissue surface. In both cases the light is modulated accordingly and the axial or lateral force can be estimated. The sensor exhibits adequate linear response, having a good working range, very good resolution and good sensitivity in both axial and lateral force directions. In addition, the use of low-cost and MR-compatible materials for its development makes the sensor safe for use inside MRI environments.**

I. Introduction

PERCUTANEOUS coronary intervention (PCI) and electrophysiology (EP) are minimally invasive procedures of the heart that are nowadays performed along existing routes inside the human body, such as blood vessels, and are carried out with the use of catheters. A catheter is a thin and flexible elongated tube that is inserted through a small incision in the groin (upper thigh), the arm, or the neck of the patient [1], where one of the main blood arteries is located. Catheter diameters are in order of several French (Fr), with one Fr being a third of a millimetre.

During a cardiac catheterisation procedure, the physician intents to reach certain locations via the blood vessels and perform examinations or treatments to tissues of the heart. This minimally invasive surgery (MIS) procedure offers many advantages, including reduced trauma to tissues, reduced recovery time, less infections and lower overall hospitalisation costs, as in every other MIS [2].

Manuscript received September 15, 2009. The first author's research studies are partially funded by the Alexander S. Onassis Public Benefit Foundation, which is based in Greece, and is greatly appreciated. The research leading to these results has received funding from the European Community's Seventh Framework Programme FP7/2007-2013 under Grant Agreement No. 231640.

Panagiotis Polygerinos, Pinyo Puangmali, Lakmal D. Seneviratne, and Kaspar Althoefer are with King's College London, Department of Mechanical Engineering, Strand, London, WC2R 2LS, UK (email: panagiotis.polygerinos@kcl.ac.uk; pinyo.puangmali@kcl.ac.uk; lakmal.seneviratne@kcl.ac.uk; k.althoefer@kcl.ac.uk).

Reza Razavi and Tobias Schaeffter are with the Division of Imaging Sciences King's College London, The Rayne Institute, St.Thomas' Hospital, London, SE1 7EH, UK (e-mail: reza.razavi@kcl.ac.uk; tobias.schaeffter@kcl.ac.uk).

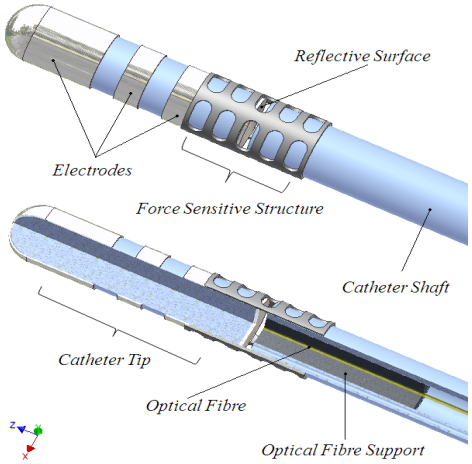

Fig. 1. CAD drawings of a 7 Fr catheter integrated with the proposed fibre-optic force sensor.

Currently, physicians make use of X-ray fluoroscopy to navigate the catheters through the patient's body. This technique involves the use of an X-ray source and a detector to obtain real-time projection images of the patient body and catheter device. It is noted that X-ray fluoroscopy emits ionizing radiation to the patient and medical staff to guide the PCI or EP procedure. This limits the interventional procedure time due to the risks of prolonged exposure to ionizing radiation. Furthermore, the quality of the returned tissue and organ images is poor. Usually, a contrast agent needs to be injected into the blood vessels or the heart in order to improve the visual ability. In large amounts that contrast agent can cause kidney failure and therefore is avoided as much as possible.

The above drawbacks have recently forced scientists to start looking for alternative imaging methods to perform cardiac catheterizations [3], [4]. One of the new methods that can provide distinct advantages over X-ray fluoroscopy is magnetic resonance imaging (MRI). MRI scanners operate with strong magnetic fields used to examine human networks of blood vessels and soft tissues without the need for a contrast agent, producing three dimensional images with superior soft tissue contrast and most importantly without emitting hazardous ionizing radiations. However, an MRI scanner encompass a main constrain. Due to the high magnetic fields, it requires non-magnetic tools and devices. Usually, two main effects have to be considered

Fig. 2. Photograph of the fibre-optic sensor prototype integrated with a 7 Fr catheter. A one GB-pound coin is shown for comparison.

for MR safety. First, the strong magnetic field can cause displacements of certain metallic materials. Secondly, conductive wires inside an MRI scanner can potentially work as MR-antennas, possibly resulting in heating effects at the tip of the wire. Therefore, magnetic and conductive materials with certain length cannot be used as they could distort the MR images, be displaced by magnetic field (projectile effect), and even heat up, putting the life of patients at risk [5]. Thus, any materials used must be non-magnetic and MR safe [6].

In this paper, a new prototype miniature catheter-tip force sensor that employs fiber-optic technology is presented. The intention is to bridge the gap between the detection of contact forces from the tissue-catheter interaction during a cardiac catheterization and the need of MRI-compatible sensors with low manufacturing cost.

II. Force Feedback in Cardiac Catheterization

Interventional cardiologists are often able to sense the interaction of the catheter with the internal structures (e.g. blood vessels and atrium of the heart) while performing a catheterization. This haptic feedback is often used by the physician to determine the position and to facilitate the manoeuvring of the catheter. The information feedback from the catheter also indicates, particularly in the case of an EP ablation, the outcome of the procedure, as a good contact of the catheter-tip assures a successful result. However, distinction between involved force components is a difficult task and requires extensive training from the side of the physician to achieve adequate expertise. The difficulty stems from the fact that the forces involved are a combination of two force components: one originates from the friction between the catheter and the blood vessel and the other from the catheter tip when in contact with the blood vessel or cardiac wall [7]. In addition, the orientation of the catheter-tip is independent and difficult to predict making any given task even more complicated.

Many types of force and pressure sensors have been developed in the past for use in catheterization procedures. These sensors were used for different kinds of measurements, such as blood pressure, oxygen level, blood flow, blood velocity and others. They make use of several sensing principles, such as strain-gauges [8], piezoresistivity [9], PVDF films [1] and fibre-optic technology [10], [11], [15]. However, only a small number of sensors were developed for the detection of contact forces between the catheter and tissue [12], [13].

III. Novel Fiber-Optic Force Sensor

A. Prototype Sensor

For this research, a plastic 7 Fr catheter tube (Fig. 1) was used. The tube is divided in two parts. The first part, the tip of the catheter, accommodates the electrodes for EP ablation and a reflective flat circular face. The occupied area of the reflective surface is equal with the catheter's cross section and is located at the opposite end of the main tip electrode. The second part is the actual flexible shaft of the catheter. The two separate parts of the catheter are connected, positioned and aligned together with a force sensitive (deformable) structure of 12 Fr, allowing a very small gap of 0.6 mm to form between them. The main shaft contains a 0.25-mm-diameter plastic optical fiber. The optical-fiber is held in position in such a way that the one end is at the same plane level where the end of the main catheter's shaft is. The remaining other end of the optical-fiber is connected with a photodiode detector.

With this configuration a light is emitted from a light source through the optical fiber onto a reflective surface and then reflected back to a photodiode. When a force is applied at the tip of the catheter, the connecting structure is deformed and modulates the light intensity that can be read out by the photodiode via an optical coupler and further interpreted as a force signal. In conjunction with the use of one imaging technique (X-rays, MRI), the prototype sensor is able to detect axial and lateral forces separately, by knowing the orientation of the catheter tip in relation to the cardiac tissue wall.

B. Light Intensity Modulation

The principle of operation of the proposed force sensor is based on the variation of the light intensity caused by the change of height h (Fig. 3) for axial force loading or rotation of the reflective surface Θ (Fig. 6) for lateral force loading and the optical-fiber end. In both cases the light is transmitted and received through the same optical fiber.

A Gaussian curve can describe, as proposed by [14], the light intensity distribution profile of the light beam. The value of the beam's intensity is a function described by the cross sectional radius of the beam. Therefore, the light intensity distribution profile can be expressed in a polar coordinate as

$$I_{(r)} = I_o e^{\left(-\frac{2r^2}{w_0^2}\right)}, \quad (1)$$

where $I_{(r)}$ is the value of the beam's intensity at a radius r, I_o is the maximum intensity at radius $r = 0$ and w_0 is the mode-field radius; thus, mode-field diameter is equal to $2w_0$. As a Gaussian curve has no boundaries and theoretically the light continues spreading to infinity, it is assumed that a boundary exists where the mode-field diameter is (i.e. radius r of the cross section is equal to w_0). Substituting in equation (1) and assuming a relative intensity of 1, a drop of the light intensity to $1/e^2 = 0.135$ from the peak value is expected.

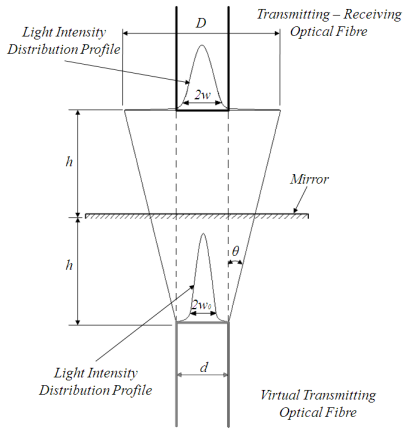

Fig. 3. Geometry of the light intensity modulation in the case of axial force loading of the sensor.

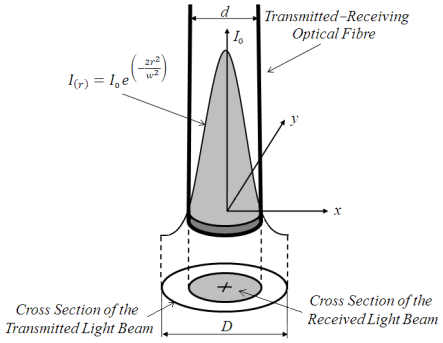

Fig. 4. Maximal transmitted light flux and actual collected light flux that is bounded by the cross section of the optical fiber with diameter *d*.

Now that the boundaries have been defined, the total flux of light can be estimated as

$$\Phi_{tran.} = \int_0^{\frac{D}{2}} I_{(r)} 2\pi r dr \approx \int_0^{\infty} I_{(r)} 2\pi r dr = \frac{I_o \pi {w_o}^2}{4}, \qquad (2)$$

where $\Phi_{tran.}$ is the total light flux which is transmitted from the optical fiber, D is the diameter of the cross sectional plane of the light intensity distribution profile at the fiber end face and $I_{(r)}$ is the current value of the beam's intensity at radius r.

1) Axial Force Loading

In the case of axial sensor loading, the optical fiber is facing the reflective surface vertically. The reflected light is received by the same optical fiber in a perpendicular manner in relation to the reflective surface. Any axial applied force reduces distance *h* between optical fiber and the reflective surface (Fig. 3). To derive the equation of the collected light flux it is imperative to know the geometry of the light when it reflects at the surface. Fig. 3 shows that the light intensity *I* drop as the distance *h* increases, but the amount of light flux always remains the same. The change of the light intensity affects only the mode-field diameter. As a consequence, it must be noted that the total light flux received by the optical fiber is not the maximum emitted light flux at a distance *h* but the flux bounded by the circular cross section of the receiving optical fiber with diameter *d,* see Fig. 4. The following equation derives the theoretical light flux able to be received by the optical fiber with *w* indicating the mode-field radius at the receiving fiber,

$$\Phi_{r,th.} = \int_0^{\frac{d}{2}} I_{(r)} 2\pi r dr = \frac{I_o \pi w^2 \left(1 - e^{-\frac{d^2}{2w^2}}\right)}{2}. \qquad (3)$$

Depending on the distance of the optical fiber from the reflective surface, the received light flux can vary and consequently the voltage output from the photodetector varies. The maximum voltage output that can be detected from the photodetector is given by

$$V_{th.} = k_v \sigma_r \int_0^{\frac{d}{2}} I_{(r)} 2\pi r dr = \frac{k_v \sigma_r I_o \pi w^2 \left(1 - e^{-\frac{d^2}{2w^2}}\right)}{2} \qquad (4)$$

where k_v transforms the received light flux of the detector into electrical signal and σ_r is the factor that represents the optical losses. These losses originate from optical fiber misalignments at the connecting points within the force sensor housing and also from optical fiber bending.

The normalized voltage output is computed from the ratio of the voltage output with the maximal voltage output that can be detected by the photo detector.

$$\frac{V_{out}}{V_{max}} = \frac{I_O w^2 \left(1 - e^{-\frac{d^2}{2w^2}}\right)}{max\left[I_O w_O^2 \left(1 - e^{-\frac{d^2}{2w_0^2}}\right)\right]} \qquad (5)$$

To validate the mathematical equations a test rig was set-up. The test rig consisted of a linear translational stage, a reflective surface (mirror) and a plastic optical fiber with a diameter of 0.25 mm, a core refractive index of 1.492 and a 61° acceptance light angle (thus, angle θ of Fig.3 and Fig.6 is 30.5°). The test rig allows varying the distance between the mirror and the tip of the optic fiber whose longitudinal axis is kept perpendicular with respect to the mirror.

The experiment was conducted three times and the initial

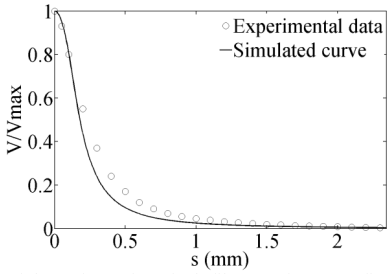

Fig. 5. Axial motion of optical fiber against a reflective surface: experimental data and simulation results (Eq. 5). The maximum error is 4.8%

distance of the optical fiber from the mirror was set to 2.5 mm; that was the distance above which no change in voltage output could be observed. Translating the stage and bringing the optical fibre closer to the mirror in steps of 0.1 mm and recording the voltage output the experimental curve of the voltage output against the distance was obtained. Using the non-linear least squares Gauss-Newton algorithm the mathematical model (Eq.5) was validated. The comparison with the experimantal data is shown in Fig. 5; a maximum error of 4.8% was observed.

2) Lateral Force Loading

When applying lateral forces, the sensor tip part is tilted with regard to the z-axis (the angle between the upper part of the catheter and the main catheter shaft changes). As the deformable connecting link between the catheter shaft and tip accepts lateral forces, the reflective surface rotates to an angle, Θ, with regard to its z-axis. This rotation changes the way the light is reflected back from reflecting surface, diverting it away from the receiving optical fiber. The geometry of the intensity distribution profile for this case can be seen in Fig. 6.

An experiment was performed to determine the amount of light that can be detected by the photodetector when an optical fiber is placed in front of a rotating mirror. During the experiment the optical fiber was kept stationary and the mirror was positioned in front of the fiber tip in such a way

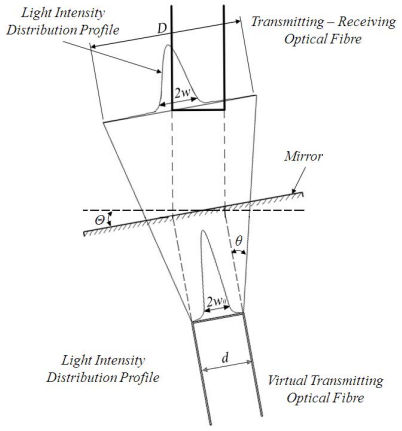

Fig. 6. Geometry of the light intensity modulation in the case of lateral force loading of the sensor. Amounts of light scatter away of the optical fibre boundaries.

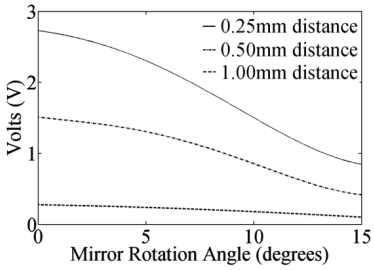

Fig. 7. Experimental data obtained rotating the mirror against the optical fibre in three different distances of 0.25, 0.5 and 1 mm.

to be able to rotate left and right above the fiber. The experiment was conducted placing the mirror in 1 mm, 0.5 mm and 0.25 mm distance, respectively from the optical fiber. For all three distances, the mirror was rotated from 0° to 15° in increments of 1° step. The voltage output was recorded and the results are illustrated in Fig. 7. From the graph, it can be observed that the sensitivity of the signal is affected by the distance between the mirror and the fiber; getting closer the mirror to the fiber, the greater the sensitivity. In addition, the voltage drop allows differentiating the axial from the lateral forces; the first yields a positive voltage signal while the second a negative one. That voltage drop increases when the angle of rotation increases.

C. Deformable Structure

In order to connect the catheter tip and the main catheter shaft, a deformable structure was needed. That structure has to be easily deformed when accepting even the smallest of axial or lateral force and, at the same time, has to be MRI-compatible. For this system, the connecting structure was made out of a monolithic silicone rubber material with a hollow cylindrical slotted shape to avoid coupling effects and to maximize the deformations due to loading. The diameter of it is 12 Fr (4 mm) and its height is 10 mm. Under axial loading, the four symmetric vertical bars (the connecting deformable parts of the catheter tip and the catheter shaft) are compressed equally minimizing the distance between optical fiber and reflective surface. On the other hand, during lateral loading, the bars are extended from the side where the force is applied and compressed at the other side, rotating the reflective surface with respect to the fiber.

The deformable structure was simulated using stress analysis software techniques to determine the amount of deformation under various axial and lateral loadings, see Fig. 8. Fig. 9 (a) and (b) show the simulation results indicating that, under axial loads up to 0.5 N, the structure is linearly deformed with a maximum deformation of 0.28 mm. Under lateral loading, the structure rotates linearly as a function of the applied force by up to an angle of 8 degrees. It must be noted that the structure is able to withstand 1 N of force before permanent damage is caused to it.

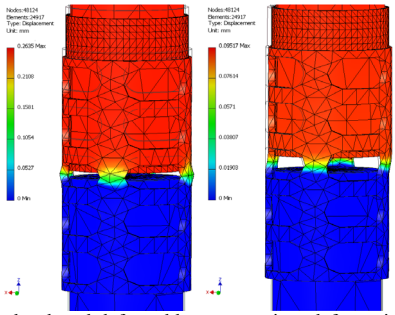

Fig. 8. The developed deformable structure in a deformation analysis using finite elements. Left: deformation of the structure in axial loading of the catheter tip. Right: deformation of the structure in lateral loading of the catheter tip.

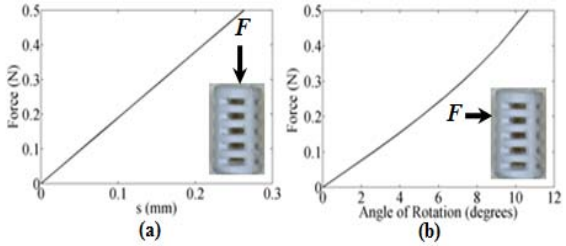

Fig. 9. (a) The simulated response of the deformable structure obtained by applying axial forces from 0 to 0.5 N (~50 grams) and (b) The simulated response of the deformable structure obtained by applying lateral force from 0 to 0.5 N (~50 grams). The lateral deflection of the structure is shown in degrees.

IV. Experiments

Experiments to calibrate and test the performance of the sensor make use of a constant red light source to transmit light with a wavelength of 650 nm through a 0.25- mm optical fiber. The light bounces on the reflective surface and is collected back from the same optical fiber which is in turn connected to a fiber-optical coupler with 50:50 splitting ratio. Through the coupler the received light signal is guided to a photodiode detector, where it is transformed to a voltage signal. The voltage signal is then amplified and filtered for noise suppression. The amplified voltage output is send through a data acquisition card to a personal computer where the signal is further managed, observed and recorded using software techniques. The schematic representation of the entire system is shown in Fig. 10.

A. Loading-Unloading Cycle

The test rig for the calibration process consists of the sensor, a rigid support to hold a linear translational stage in vertical position and an electronic scale. The developed sensor was mounted onto the linear stage vertically facing the electronic scale. The linear stage was able to move the catheter up and down. Forces exerted on the tip of the sensor as pressing it against the scale were measured. Increased vertical displacement of the stage in negative (downward) direction corresponded into increased force exertion on the electronic scale. During the experiments the load on the sensor was increased in increments of 5 grams and the voltage output signal from the sensor was recorded. When 0.5 N of force was reached the linear stage moved back decreasing the load again in increments of 5 grams. The same protocol was applied laterally loading the sensor. This time a lateral force was applied to the tip of the sensor and measured by the scale. The experiments were repeated five times to verify the repeatability of the sensor. The sensor loading and unloading curves proved to be relatively linear with small hysteresis, Fig.11.

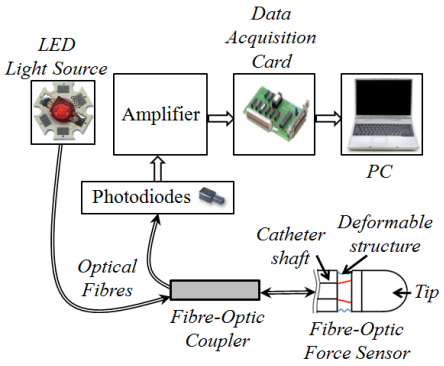

Fig. 10. Schematic diagram of operation of the miniaturized fiber-optic force sensor.

Under axial loading the sensor has a sensitivity of 1.9 V/N, a linear working range of 0.5 N ranging from 0 to 0.5 N ($R^2 = 0.9965$) and a resolution of 0.008 N. Under lateral loading it has an orientation dependent sensitivity possibly due to assembly misalignments; the sensor sensitivity varies from 3.0 V/N to 3.5 V/N depending on the side where the contact force is applied. The force working range is relatively linear from 0 to 0.5 N ($R^2 = 0.9739$) and the resolution is approximately 0.004 N. The experimental results clearly show that the sensor is best operated in the range from 0 to 0.6 mm (relatively linear region). A mirror distance of 0.6 mm or higher will result in non-linear behaviour and, in this region, the light intensity changes is small and more difficult to interpret. It is also noted that slight deviations from the perfect normal position or the perfect tangential position will still result in good estimates of the forces.

B. Silicone Tests

In order to investigate the behavior of the force sensor in interventional procedure condition further experiments were performed to simulate the motion of the catheter if moved by the hand of a physician.

During these experiments the catheter was attached to a slim rod. The catheter tip was left to stand free 20 mm out of the rod's length while its other end was rigidly connected to a force sensor, ATI nano17 (ATI Industrial Automation, Inc., NC, USA). The aim was to compare the force output response of the developed force sensor to the force outputs of the force sensor whilst being subjected to the same dynamic loading and unloading conditions.

During a first experiment, Fig.12, the developed sensor was held by a human vertically above a silicone block simulating the tissue of the heart. The catheter tip was

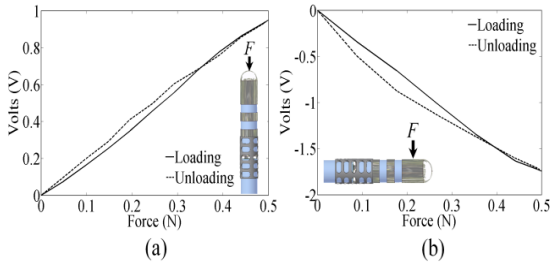

Fig. 11. Loading-unloading axial (a) and lateral (b) cycles. The hysteresis of the developed sensor that is caused by the rubber silicone material can be seen.

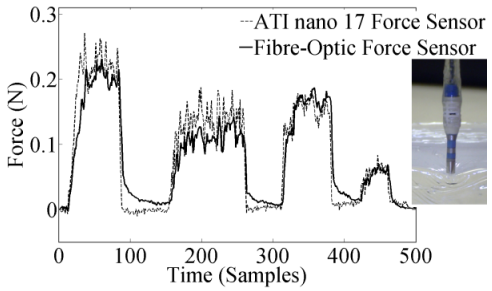

Fig. 12. Dynamic axial response of the force sensor when the catheter is pressed against a silicone block four times randomly by hand. The force results are compared with the response of a commercial force sensor.

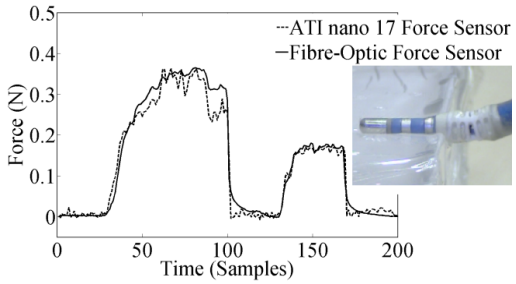

Fig. 13. Dynamic lateral response of the force sensor when the catheter is pressed against a silicone block two times randomly by hand. The force results are compared with the response of a commercial force sensor.

moved to touch the silicone block several times to mimic the EP ablation procedure, where the physician touches the tissue and performs a burn. The force output signals from both sensors are shown in Fig. 12. The experiment was repeated for lateral loading by pressing the catheter tip parallel to the surface of the silicone block such that the lateral forces applied to both sensors could be compared; Fig. 13. These experiments show that the developed tip sensor can detect forces under axial or lateral loading and unloading conditions. It was found that the results of the developed fiber-optic sensor matched the results of the commercial force sensor very well.

V. Conclusion

This paper reports the preliminary findings of a miniature prototype force sensor that was developed and integrated with a 7 Fr EP ablation catheter to tackle the lack of force feedback that physicians encounter during cardiac catheterization. The sensor employs a single optical fiber, a reflective surface and a deformable structure. One optical fiber was used to save space inside the already constrained catheter shaft space, to keep the manufacturing cost low and to decrease the complexity of the entire system. Through that design the sensor is able to detect the interaction between axial or lateral forces of the catheter tip and tissue only when an assistive imaging technique is indicating the orientation of the tip. Deformation of the sensor's structure modulates the light intensity making it possible to determine the applied forces. The materials used for the development of the sensor make it MR-compatible and thus safe for use inside MRI environments. Calibration and further experiments in soft tissue effigies returned satisfying results proving the feasibility of this low-cost force sensor prototype. More detailed experiments, clinical trials and improvements are required. However, this paper shows that fiber optic sensors have the potential to be used in such minimally invasive procedures.

References

[1] F. WeiXing, W. HuanRan, G. ShuXiang, W. KeJun, Y. XiuFen, "Design and experiments of a catheter side wall tactile sensor for minimum invasive surgery", *Int. Conf. on Mechatronics and Automation,* Harbin, 2007, pp.1073-1078.

[2] P. Puangmali, K. Althoefer, L. D. Seneviratne, D. Murphy, and P. Dasgupta, "State-of-the-art in force and tactile sensing for minimallyinvasive surgery", *IEEE Sensors Journal*, vol. 8, no. 4, pp. 371-381, Apr. 2008.

[3] V. Muthurangu, R. S. Razavi, "The value of magnetic resonance guided cardiaccatheterisation", *Heart*, vol. 91, pp. 995-996, 2005.

[4] R. Razavi, D.L.Hill, S.F. Keevil, M.E. Miquel, V. Muthurangu, S. Hegde, K. Rhode, M. Barnett, J. van Vaals, D.J. Hawkes, E. Baker, "Cardiac catheterisation guided by MRI in children and adults with congenital heart disease." *Lancet,* vol. 362, pp.1877-82, 2003.

[5] N. Yu, R. Riener. "Review on MR-compatible robotic systems." *The First IEEE/RAS-EMBS International Conference on Biomedical Robotics and Biomechatronics,* Pisa, Italy, 2006, pp. 661-665.

[6] R. Gassert, R. Moser, E. Burdet, H. Bleuler, "MRI/fMRI-compatible robotic system with force feedback for interaction with human motion", *IEEE/ASME Trans. on Mechatr.*, vol. 11, no. 2, pp. 216-224, 2006.

[7] T. Katsumata, Y. Haga,, K. Minami, M. Esashi. "Micromachined 125μm diameter ultra miniature fibre-optic pressure sensor for catheter." *Transactions IEE Japan*, vol. 120, no.2, pp. 58-63, 2000.

[8] H. Allen, K. Ramzan, J. Knutti, S. Withers, "A novel ultra-miniature catheter tip pressure sensor fabricated using silicon and glass thinning techniques." *MRS Conf.,* San Francisco, CA, 2001, pp. I7.4.

[9] D. Tanase, JFL. Goosen, P.J. Trimp, , PJ. French, "Multi-parameter sensor system with intravascular navigation for catheter/guide wire application." *Sensors and Actuators,* pp. 116-124, 2002.

[10] C. Strandman, L. Smithb, L. Tenerzb, B. Hök, "A production process of silicon sensor elements for a fibre-optic pressure sensor." *Sensors and Actuators,* vol.63, no.1, pp.69-74, 1997.

[11] E. Cibula, D. Donlagic, C. Stropnik, "Miniature fiber optic pressure sensor for medical applications." in *Proc. of IEEE Sens.,* pp.711-714, 2002.

[12] K. Yokoyama, H. Nakagawa, D.C. Shah, H. Lambert, G. Leo, N. Aeby, A. Ikeda, J.V. Pitha, T. Sharma, R. Lazzara, W. M. Jackman. "Novel contact force sensor incorporated in irrigated radiofrequency ablation catheter predicts lesion size and incidence of steam pop and thrombus." *Circulation: Arrhythmia and Electrophysiology, v*ol. 1, no. 5, pp. 354-362, Dec. 2008.

[13] P. Polygerinos, T. Schaeffter, L. D. Seneviratne, K. Althoefer, "A fibre-optic catheter-tip force sensor with MRI compatibility: A feasibility study", in *Conf. Proc. IEEE Eng. Med. Biol. Soc.*, Minneapolis, MN, 2009, pp.1501-1504.

[14] P. Puangmali, K. Althoefer, L.D. Seneviratne, "Mathematical modeling of intensity-modulated bent-tip optical fiber displacement sensors", *IEEE Trans. Instrum. Meas*., vol. 59, no. 2, Feb. 2010.

[15] D. P. Noonan, H. Liu, Y. H. Zweiri, K. A. Althoefer, L. D. Seneviratne, "A dual-function wheeled probe for tissue viscoelastic property identification during minimally invasive surgery", in *Proc. IEEE Int. Conf. Robot. Autom.,* Roma, Italy, 2007, pp. 2629-2634.